International Journal of Latest Research in Science and Technology **ISSN (Online):2278-5299**
Volume 3, Issue 1: Page No.9-13 ,January-February 2014
https://www.mnkpublication.com/journal/ijlrst/index.php

A UNIFIED OPTIMALIZATION THEORY FOR PHOTO-INITIATED MEDICAL APPLICATIONS

Jui-Teng Lin
New Vision Inc. Taipei, Taiwan

Abstract- A unified theory and its medical applications in photothermal and photochemical systems are presented. The double-optimal conditions for the largest flat-profile depth, characterized by small absorption and long focal length, provide useful clinical guidance for efficient photo-initiated therapy, particularly for large volume medium.

Keywords **-** Photothermal; Photochemical; Biomedical systems; Modeling; Optimalization

I. INTRODUCTION

One of the critical issues in light-induced biometical processes is how to improve the uniform temperature profile in photothermal systems [1] or the initiator concentration in phtotochemical systems [2-4]. In addition to the need for large light penetration depth in the absorbing medium. Near infrared (NIR) lasers have been commonly used in various therapy systems in replacing the visible lasers which has a much shallow penetration depth in soft tissues [1]. For example, nanogolds in rod-shape [5] or in core-shell [6] are used as the initiator for cancer therapy using a diode laser at about 810 nm in contrast to the use of spherical nanogold using a green laser at about 532 nm [7].

In photo-initiated systems under a collimated light (lasers or LEDs), the intrinsic drawback is that the photo-initiated processes always start from the entrance (or surface) portion of the absorbing medium. In other words, the process is faster on the surface than the volume. Therefore, non-uniform profiles (temperature or concentration) inside the medium always occur in collimated light having an exponentially deceasing intensity profile as referred as the Beer's law.

In this study, I will present the new concept using a focused-beam to achieve uniform profiles and larger penetration depth under double-optimal conditions defined by the absorption coefficient of the medium and focal length of the light. Large penetration is particularly important for the treatment of large size (or thickness) of photo-initiated medium.

I will first introduce the concept and the advantage of a focused-beam comparing to a collimated beam. We will then solve the heat diffusion equation to obtain the temperature profiles and to define the optimal focal length and absorption coefficient for flat-profile depth.

As a second medical model, I will present a photo-initiated polymerization system, where the initiator concentration profiles will be optimized for uniformity and maximal penetration. Finally, a unified theory based on a common light source term presenting the optimal condition for both photothermal and photochemical systems is presented.

II. THE MEDICAL MODELS

Two major photo-initiated biomedical processes are described as follows.

(a) Photothermal processes such as: cancer therapy using nanogold as the absorbing initiator under a NIR laser [1]; thermal lasers for cosmetic applications; thermal lasers for coagulation of ablation of soft tissues in dental and ophthalmic clinics etc. The key parameters in these processes include the laser intensity, irradiation period, medium absorption coefficient at the specified light wavelength, laser operation modes (cw or pulsed), where the efficacy of the processes is governed by the temperature increase of the treated medium.

(b) Photochemical processes such as: UV-light-induced cross linking of corneal collagen [2]; LED light curing and photodynamic therapy (PDT) in dental clinic; photo-initiated polymerization of biomaterials for tissue re-engineering [8,9] etc. The key parameters in these processes are similar to phtothermal processes, except that the efficacy of the processes is governed by the time dependent profile of the initiator concentration.

The above described two processes may be mathematically model by a heat diffusion equation (for Photothermal), and a coupled kinetic equation (fro photochemical) to be further detailed as follows.

A general model system is shown in Fig. 1, where a laser (or light) is focused into an absorbing medium along the depth (z) of the medium. The laser fluence of a focused beam may be expressed by an analytic form of

$$F_1(z) = F\left(1 - \frac{1-r}{f} z\right)^{-2} \quad \text{, for z<f,} \qquad (1.a)$$

$$F_1(z) = F\left(r + \frac{1-r}{f}(z-f)\right)^{-2} \quad \text{for z>f.} \qquad (1.b)$$

Where r is a ratio between the beam spot size at the entrance plan (z=0) and at the focal point (z=f); and F is the laser

Publication History
Manuscript Received : 8 January 2014
Manuscript Accepted : 28 January 2014
Revision Received : 29 January 2014
Manuscript Published : 28 February 2014

fluence at the entrance plan (z=0). In general, the r value depends on the beam divergent angle and beam quality of the collimated laser. In our calculations, we will use r=0.2

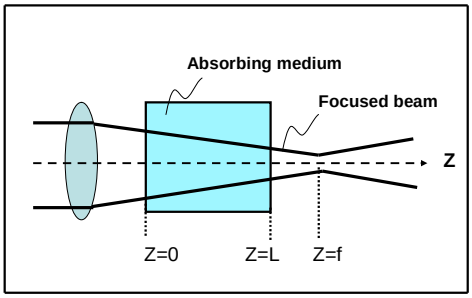

Fig. 1 Schematic of a focused laser beam propagates along the z-direction (the depth of an absorbing medium) having a focal length (f) which defines a short (dashed curve) and a long focusing (solid curve).

A. The Photothermal System

The temperature increase of an absorbing medium due to laser heating may be described by a one-dimensional heat diffusion equation [1]

$$\frac{\partial^2 T}{\partial z^2} - \frac{1}{k}\frac{\partial T}{\partial t} = -S(z) \quad , \qquad (2.a)$$

where the laser heating source term is given by

$$S(z) = \frac{AF_1(z)}{K} e^{-Bz} \quad . \qquad (2.b)$$

Where k and K are, respectively, the thermal conductivity and diffusivity of the tumor. B is the extinction coefficient of the absorbing medium consisting of two components: B= [A (A+2b)]1/2, where A and b are the absorption and scattering coefficient. In this study we will focus on the role of the absorption term (A), with b<<A such that that B=A in our calculations.

The above heat diffusion equation can be solved numerically under the initial condition $T(z,0)=T_0$, and the boundary condition

$$\left(\frac{\partial T}{\partial z}\right)_{z=0} = \frac{h}{K}\left[T(t, z=0) - T_0\right] \qquad (2.c)$$

In Eq. (2.c), h is the heat transport coefficient due to the air convection of the medium surface. We will focus on the features of a focused-beam and assume an isolated surface, or for h=0. Typical parameters to be used in our calculations are [1] k=0.00149 (W/C/cm), K=0.0045 (cm^2/s).

B. The Photochemical Systems

For a thick medium illuminated by a UV laser, the molar concentration of the photoinitiator C(z,t) and the UV laser fluence (or intensity) I(z,t) may be described by a one dimensional kinetic model as follows [2].

$$\frac{\partial C(z,t)}{\partial t} = -aI(z,t)F_1(z)C(z,t) \qquad (3.a)$$

$$\frac{\partial I(z,t)}{\partial z} = -2.303\varepsilon_1 C(z,t)I(z,t) \qquad (3.b)$$

Where $F_1(z)$ is the focusing function defined by Eq. (1); C_0 is the initial value, $C_0 = C(z, t=0)$; and $a = 83.6\lambda\phi\varepsilon_1$, with ϕ being the quantum yield and λ being the laser wavelength; and ε_1 is the molar extinction coefficient of the initiator and the photolysis product, respectively. In our calculations, the following units are used: $C(z,t)$ in mM, F(z,t) in (mW/cm^2), λ in cm, z in cm, in second, and ε_j in $(mM\cdot cm)^{-1}$. In Eq. (3), we have ignored the absorption due to the photolysis product or the medium without the initiator.

We note that the kinetic equation (3) and the heat diffusion equation (1) can be related by a unified light source term by re-formulating Eq. (3.a) as following

$$\frac{\partial C(z,t)}{\partial t} = -S'(z,t) \qquad (4.a)$$

where the light source term, comparing to Eq. (2.b), is given by

$$S'(z,t) = aI(z,t)C(z,t)F_1(z)/F \qquad (4.b)$$

where the laser intensity has an initial value of $I(z,0)=I_0$ in the case of collimated beam.

For the case of collimated beam (with $F_1=F$), analytic solution of Eq. (3) is available and is given by [10]

$$C(z,t) = C_0 / \left[1 + (e^X - 1)e^{-Y}\right] \qquad (5)$$

where $X = aI_0 t$, $Y = bC_0 z$, $b = 2.3\varepsilon_1$. As expected for t=0, $C(z,0)=C_0$, and at z=0, C(0,t)=exp(-X), for steady-state, X>>1, C(z,s.s)= 0. Numerical simulations are required for the focused beam.

In addition, the absorption coefficient (A) in Eq. (2) is related to the molar extinction coefficient and the initiator concentration by $A = 2.3\varepsilon_1 C_0$. Therefore Y=Az.

One may also relate the above source term S'(z,t) to the photoinitiation rate of production of free radicals, *R(z,t)*, by (for the collimated case)

$$S'(z,t) = 41.8\lambda R(z,t) \qquad (6)$$

By symmetric argument, one may easily solve for I(z,t) based on Eq. (5), for the collimated case, and obtain the analytic formulas for S'(z,t), or the rate function R(z,t),

$$S'(z,t) = \frac{81.6\lambda\phi(\varepsilon_1 C_0 I_0)}{\left[1 + (e^Y - 1)e^{-X}\right]\left[1 + (e^X - 1)e^{-Y}\right]} \qquad (7)$$

In the first order approximation, one may obtain

$$S'(z,t) = 83.8\lambda\phi(\varepsilon_1 C_0) I_0 \exp\left[-2.3(\varepsilon_1 C_0)z - X\right] \qquad (8.a)$$

Using $A = 2.3\varepsilon_1 C_0$ Eq. (8.a) becomes

$$S'(z) = (35.5\lambda\phi)AI_0 \exp[-Az] \qquad (8.b)$$

which has the same format as Eq. (2.b) for the collimated case with $F_1(z)=F$.

III. OPTIMALIZATION

Double optimalization based on the absorption coefficient (for collimated beam) and the focal length (for focused beam) are discussed as follows.

A. The Collimated case

The light source terms S(z) and S'(z) given by Eq. (2.b) and Eq. (8.b), have a common feature of optimalization. By taking dS/dA (A=A*)=0, or dS'/dA (A=A*)=0, one obtains the maximal S (or S') under the optimal condition A*=1/z. The maximal S (or S') is resulted from the competing function of A and exp(-Az). Fig. 3 shows S(z) vs. As shown by Fig. 2 and 3 for the photothermal case based on Eq. (2.b) and photochemical case based on Eq. (6) and (7) demonstrate the optimal A* is inverse proportional to z.

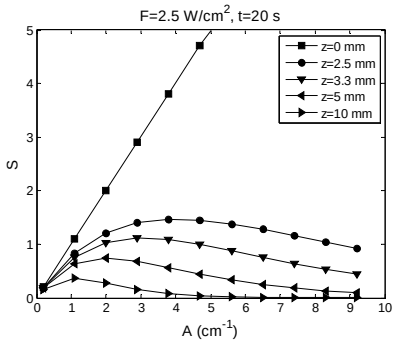

Fig. 2 The profiles of the source term S(z) at various z. where, for z>0, maximum S (z) at the optimal absorption coefficient given by A*=1/z.

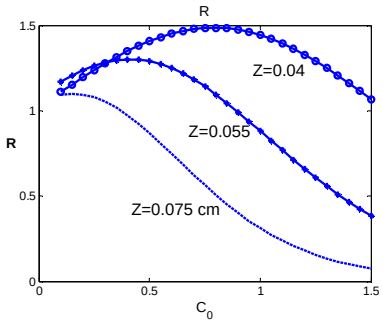

Fig. 3 The photoinitiation rate R(z,t) versus the photoinitiator initial concentration at a given time t=20 second for a light intensity I_0=10 mW/cm^2, at various z=0.025, 0.055 and 0.04 cm.

B. The Focused Case

The second optimal condition is based on the optimal focal length (f*) such that the uniform temperature profile (in photothermal system) or initiator concentration (in phtotochemical system) may be achieved. These uniform profiles are the unique feature of focused beam and not available in collimated beam.

Figure 4 shows the profile of the source term (S) for fixed value of A=1.0 (1/cm) and F=2.5 (W/cm^2), for various focal length f=1.8 cm (tightly focused beam) to f=100 cm (the highly collimated beam). It can be easily seen that up to the absorbing depth of z=1.0 cm, the S profile for tightly focused case have higher volume value (z>0) than the surface value (at z=0), in contrast to that of the collimated beam which shows an exponentially deceasing function having its maximum always on the surface (at z=0).

As demonstrated by Fig. 4, the focused-beam technique could achieve almost flat and uniform profiles up to a flat-profile depth of z*=0.4, 0.5 and 1.0 cm, for a focal length of f=1.8, 2.0 and 2.2 cm, respectively. These optimal focal length (f*) is inverse proportional to the flat-profile depth (z*). In other words, one should use a longer focal length to achieve a large flat-profile-depth z*.

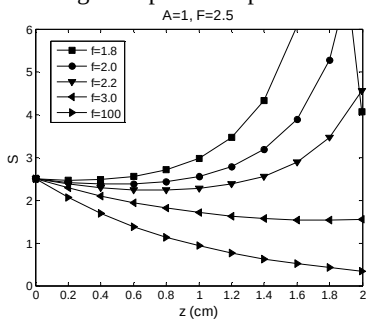

Fig. 4 Profiles of the source term for fixed value of A=1.0 (1/cm) and F=2.5 (W/cm2), at various focal length f=1.8 cm (a tightly focused beam) and f=100 cm (a highly collimated beam).

The heat diffusion equation is numerically solved to obtain the temperature profiles show in Figure 5, for the case of A=1.0 (1/cm) and F=2.5 (W/cm2), and for initial temperature of 25^0 C and an irradiation time of 20 seconds. Figure 5 shows the temperature profiles for higher value A=2.0 (1/cm) at various focal length f=1.8 cm to 100 cm, associate with the source profile shown in Fig. 4. The temperature profiles shown in Fig. 5 has the similar features as that of the source profiles (Fig. 4).

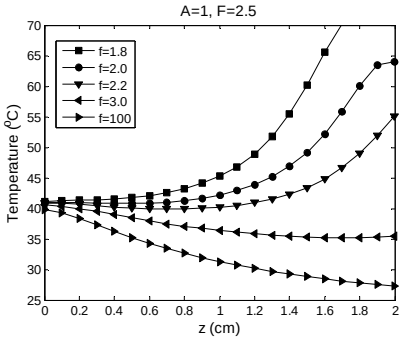

Fig. 5 Temperature profiles for A=1.0 (1/cm) and F=2.5 (W/cm2) at various focal length f=1.8 cm to 100 cm, associate with the source profile (see Fig. 2).

C. The optimal focal length

For the source term profiles, I have shown the optimal focal length is inverse proportional to the source term flat-profile depth (z*). This feature is also achieved in the

temperature profiles. As demonstrated by Figure 6, for a fixed laser fluence but various focal length and A values. We should note that all profiles are compared under the same product of fA=2.0. These temperature profiles have a cutoff flat-profile depths position (indicated by arrows) which are inverse proportional to the absorption coefficient (A value), but proportional to the focal length (f).

It should be noted that the simple relation of optimal condition A*=1/z for the source term S(z) is also approximately met for the temperature profiles of focused beams. The z-dependence of the source term and the temperature is much more complex than that of collimated beam and could only be solved numerically. As shown by Figure 5, the temperature flat-profile depth at z*=0.4, 0.6, 0.9, and 1.4 cm having the associate A values (shown in Figure 5) A=2.0, 1.5, 1.0 and 0.66 (1/cm) which meet approximately the optimal source term relation of A=1/z*.

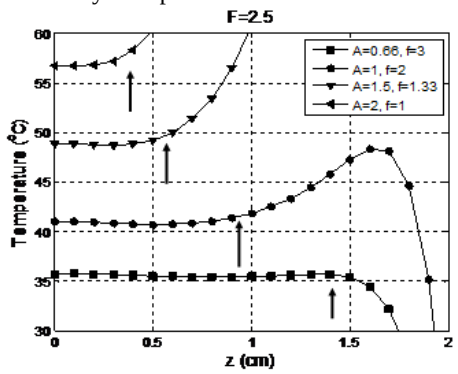

Fig. 6 The flat temperature profiles for a fixed laser fluence but for various A and f (with a fixed product of Af=2.0).

The double optimal conditions for the largest flat-profile depth (z*), characterized by small A and long focal length (f), provide useful clinical guidance fro efficient laser therapy particularly for large volume medium. Smaller A value provides a larger flat-profile depth (z*), it however also has a lower temperature increase, for a given irradiation time and laser fluence. This tradeoff may be compensated by either using a higher laser fluence or a longer irradiation time. That is to say, one could either select the laser wavelength or control the absorption of the medium to achieve the maximum flat-profile depth, in addition to the control of optimal focal length.

D. The Photochemical Systems

(1) The optimal concentration

In Fig. 7, a focused UV laser with a focal length f=2.0 cm is used to suppress the increasing profiles of C(z,t) such that a more uniform distribution (along the medium thickness direction z) may be achieved. It may be seen that f=2.0 cm is an optimized focal length for almost uniform C (z,t) along the z-direction, up to the medium thickness L=1.5 cm. However, it is only apply to the profile of C_0 =2.0 mM. It is too much focused for smaller C_0 <2.0 mM and not enough for large C_0 >2.5 mM. In other words, shorter focal length is needed for larger C_0

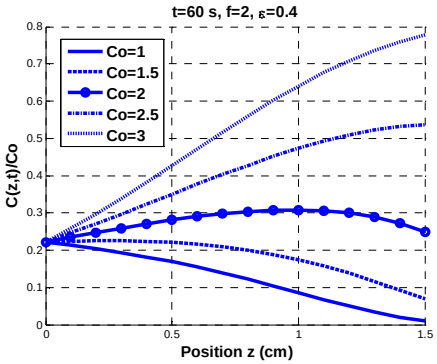

Fig. 7. Profiles of normalized initiator concentration $C(z,t)/C_0$ for a focused beam (with focal length f=2.0 cm), at t=60 seconds and a given extinction coefficient of the initiator ε_1 =0.4 (mM·cm)$^{-1}$, for various initial concentration C_0 = 1.0 to 3.0 mM

(2) The optimal focal length

As shown by Figure 8, the profiles of C(z,t) are calculated for various degree of focusing, for a given ε_1 =0.4 (mM·cm)$^{-1}$, t=60 seconds and C_0 =1.0 mM. The optimal focal lengths (f*) are defined as when C(z,t=60 s) profiles reach the most uniform distributions along the z direction. Our numerical solutions show that f*=(3.3, 2.5, 2.0, 1.6, 1.3, 1.15, 1.0) cm, for C_0 =(1.0, 1.5, 2.0, 2.5, 3.0, 3.5, 4.0) mM, with ε_1 =0.4 (mM·cm)$^{-1}$ and at t=60 seconds. These calculated f* may be fit to a scaling law equation given by $f^* = 1.6/(\varepsilon_1 C_0)$. This scaling law based on the numerical calculation was also discussed based on our earlier analytic formulas,

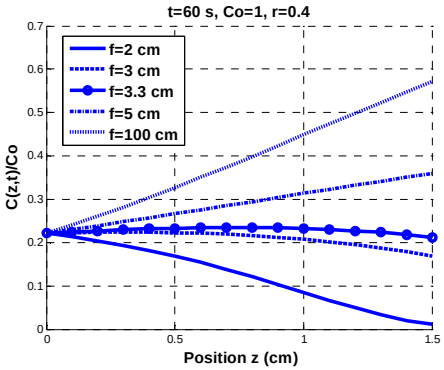

Fig. 8. Profiles of normalized initiator concentration $C(z,t)/C_0$ for focused beam having various focal length at t=60 seconds and a given extinction coefficient of the initiator ε_1 =0.4 (mM·cm)$^{-1}$. The profiles produced by optimal focal lengths are shown by dotted curves.

(3) The polymerization boundary

The above discussed polymerization boundary for various focusing conditions is further demonstrated by Figure 9, which shows the schematics of time evolution (at t=50 and 60 seconds) of photo-polymerization via: (1) collimated beam, (2) tightly focused (with F=L), (3) optimal focusing (f=f*), and (4) slightly focusing (f=2L), where the polymerized

portions are shown by shaded areas and the un-polymerized areas are shown by white areas. This schematic is further interpreted as follows.

For a collimated beam, the top portion (about 0.3 cm) of the medium is always polymerized starting from the surface (z=0) which has the highest polymerization rate and the deep portion (z>0.6 cm) remains un-polymerized.

For a tightly focused case (with f=L=1.5 cm), the medium is polymerized starting from the bottom portion which has a higher laser intensity initially, and therefore initiator concentration C(z,t) is depleted faster than the top portion. For a slightly focused case (with f=2L>f*, not optimized), the polymerization process of collimated case is improved, but not enough. At the optimal focusing, with f=f* given by the scaling law, the photo-polymerization process starts from both ends (top and bottom)and gradually move to the central portion until the whole medium is polymerized.

The tightly focused, case (2) in Fig. 9 with f=L, provide the fastest process than others. However, the optimized case (3) with f=f*, provides a larger volume of completed polymerization at a given time. We choose f* as the optimal condition based on not only the uniform polymerization distribution, but also by its large volume than the tighter focusing case.

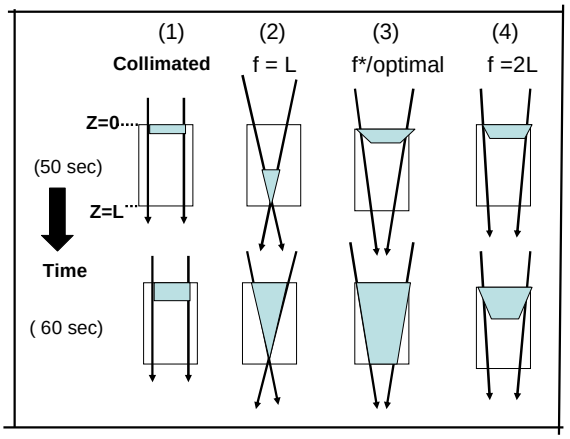

Fig. 9. Schematics of time evolution of photo-polymerization via: (1) collimated beam, (2) tightly focused (with F=L), (3) optimal focusing (f=f*), and (4) slightly focusing (f=2L), where the polymerized portions are shown by shaded areas (after J. T. Lin, D. C. Cheng and H.W. Liu [11]).

III.CONCLUSIONS

In this study, I have numerically demonstrated, in a photothermal system, flat-temperature profiles are achievable under a set of optimal condition given by the absorption coefficient (A) and the focal length (f). For a large flat-profile depth, one requires a small A value, but a long focal length and a high laser fluence to shorten the irradiation time needed. The double optimal conditions for the largest flat-profile depth (z*), characterized by small A and long focal length (f), provide useful clinical guidance for efficient cancer therapy particularly for large volume medium..

It was also presented by a comprehensive modeling for the kinetic of UV laser photoinitiated polymerization in thick polymer system. I have demonstrated that the focused beam at an optimal condition (f=f*) achieves uniform polymerization and eliminates the intrinsic drawback of collimated beam in thick medium. Transient profiles of the initiator concentration at various focusing conditions are analyzed to define the polymerization boundary and to demonstrate the advantage of optimal focusing for more uniform polymerization and larger volume than the collimated or non-optimal cases. Too much focusing (with f<f*) provides fast process, however, it has a smaller polymerization volume at a given time than the optimal focusing case.

Finally, a scaling law governed by $f^* = 1.6/(\varepsilon_1 C_0)$ is derived numerically and shows that larger extinction coefficient or larger initial concentration of the initiator, that is larger value of ($\varepsilon_1 C_0$) requires a tighter focusing, or a smaller f*. The scaling law provides useful guidance for the prediction of the photoinitiated polymerization particularly in thick polymer systems under a focused UV laser illumination. The focusing technique also provides a novel and unique means for uniform photopolymerization (within a limited time of light irradiation) which can not be achieved by any others means.

ACKNOWLEDGMENT

This work was partially supported by by the grant from Xiamen-200 program (Xiamen Science & Technology Bureau, China).

REFERENCES

[1] Lin, J. T., Chiang, S., Lin G. H. , Lee, Liu, W. H., "In vitro photothermal destruction of cancer cells using gold nanorods and pulsed-train near-infrared laser", J. Nanomaterials vol. 2012, article ID 861385, (2012).

[2] Lin, J. T., Liu, H. W., Cheng, D. C., "On the critical issues of UV light corneal cross linking", Journal of Medical and Biological Engineering, doi:10.5405/jmbe.1532,2013.

[3] Odian, O., editor. Principles of Polymerization. New York: Wiley, 1991.

[4] Fouassier, J-P., Photoinitiation, Photopolymerization, and Photocuring: Fundamentals and Applications. Munich: Carl Hanser Verlag, 1995.

[5] Lin, J. T. "Nonlinear optical theory and figure of merit of surface plasmon resonance of gold nanorods", J. Nanophotonics vol. 5, p. 051506, 2011.

[6] Lin, J. T., "Scaling law and figure of merit of biosensor using gold nanoshells". J Nanophotonics, Vol.4, 049507 , 2010.

[7] Lin, J. T., "A generalized geometric factor for unified scaling law for bio-sensor based on nanostructures of gold", Inter J Latest Res Science and Tech, vol.xx, pp. XX, 2013, (in press).

[8] Hu, J., Hou, Y., Park, H., Choi, B., et al, "Visible light crosslinkable chitosan hydrogels for tissue engineering", Acta Biomaterialia. Vol. 8, pp. 1730-1738, 2012.

[9] Tirella, A., Liberto, T., Ahluwalia. A., "Riboflavin and collagen: new crosslinking methods to tailor the stiffness of hydrogels." Materials Letters 74, pp. 58-61, 2012.

[10] Terrones, g., Pearlstein, A. J., "Effects of optical attenuation and consumption of a photobleaching initiator on local initiation rates in photopolymerrizations. Macromolecules, vol. 34, pp. 3195-3204,2001.

[11] Lin, J. T., Cheng, D. C., Liu, H. W., "A unified Analysis for double optimal conditions in photothermal and photochemical biomedical systems", Proc. I nt. Conf. on Complex Medical Engineering (IEEE CME), June 26-29, 2014 (in press).